

Adaptive Backstepping Control of a Bicopter in Pure Feedback Form with Dynamic Extension

Jhon Manuel Portella Delgado, Mohammad Mirtaba, and Ankit Goel

Abstract—This paper presents a model-based, adaptive, nonlinear controller for the bicopter stabilization and trajectory-tracking problem. The nonlinear controller is designed using the backstepping technique. Due to the non-invertibility of the input map, the bicopter system is first dynamically extended. However, the resulting dynamically extended system is in the pure feedback form with the uncertainty appearing in the input map. The adaptive backstepping technique is then extended and applied to design the controller. The proposed controller is validated in simulation for a smooth and nonsmooth trajectory-tracking problem.

keywords: adaptive backstepping control, dynamic extension, bicopter, multicopter.

I. INTRODUCTION

Multicopters have been widely used in several engineering applications such as precision agriculture [1], environmental survey [2], [3], construction management [4] and load transportation [5]. This popularity has also sparked interest in broadening their capacities and applications. Nonetheless, due to nonlinear, time-varying, unmodeled dynamics, unknown operating environments, and evermore demanding applications, reliable multicopter control remains a challenging problem.

Various control techniques have been applied to design control systems for multicopters [6]–[8]. Nevertheless, these techniques require prior knowledge of model parameters and, thus, are sensitive to physical model parameter uncertainty [9], [10]. Several adaptive control techniques have been applied to address the problem of unmodeled, unknown, and uncertain dynamics, such as model reference adaptive control [11], [12], L1 adaptive control [13], adaptive sliding mode control [14]–[16], retrospective cost adaptive control [17], [18]. These approaches either require an existing stabilizing controller or do not provide stability guarantees.

Modern control architectures decompose the multicopter’s nonlinear dynamics into outer-loop translational dynamics and the inner-loop rotational dynamics [19]. Note that the translation dynamics is linear and the

rotational dynamics is nonlinear. Stabilizing controllers are then designed for each loop separately. However, the cascaded multiloop architecture does not guarantee the stability of the entire closed-loop system. The multiloop architecture is motivated by the time separation principle, which is applicable in a scenario where each successive inner feedback loop is sufficiently faster than the previous outer loop. A stabilizing controller can be designed for each loop with appropriate transient behavior in such a case to satisfy the time separation principle. This crucial fact allows the multicopter dynamics to be decoupled and stabilizing controllers designed for each loop. Although the controller design is considerably simplified, the closed-loop stability can not be guaranteed.

This paper considers the problem of designing an adaptive controller for the fully coupled nonlinear dynamics of a multicopter. To focus on the controller design process, we consider a bicopter system, which is special case of a multicopter system. A bicopter is constrained to a vertical plane and thus is modeled by a 6th-order nonlinear instead of a 12th-order nonlinear system. Despite the lower dimension of the state space, the 6th-order bicopter retains the complexities of the nonlinear dynamics of an unconstrained multicopter. In this paper, we design an adaptive controller based on the backstepping technique [20]. However, the classical backstepping technique can not be applied due to the input map’s non invertibility. To circumvent this problem, the bicopter dynamics is first dynamically extended [21] Although the input map of the resulting extended system is invertible, the extended dynamics can only be expressed in the pure feedback form. Backstepping technique has been extended to design controllers for a system in pure feedback form in [22]–[24]. An adaptive extension of the backstepping technique for a pure feedback system was presented in [25]. However, [25] considers the case where uncertainty is in the dynamics map. As shown in Section III-B, the uncertainty in the bicopter dynamics appears in the input map. The contributions of this paper are thus 1) the design of an adaptive backstepping controller for the fully nonlinear bicopter system without decoupling the nonlinear system into simpler subsystems 2) extension of the backstepping control of pure feedback system to the case of uncertain

Jhon Manuel Portella Delgado and Mohammad Mirtaba are graduate students in the Department of Mechanical Engineering, University of Maryland, Baltimore County, 1000 Hilltop Circle, Baltimore, MD 21250. jportella@umbc.edu, mmirtabl@umbc.edu

Ankit Goel is an Assistant Professor in the Department of Mechanical Engineering, University of Maryland, Baltimore County, 1000 Hilltop Circle, Baltimore, MD 21250. ankgoe1@umbc.edu

input maps, and 3) validation of the proposed controller in a smooth and nonsmooth trajectory-tracking problem.

The paper is organized as follows. Section II derives the equation of motion of the bicopter system. Section III describes the adaptive backstepping procedure to design the adaptive controller for the bicopter. Section IV describes a numerical simulation to validate the adaptive controller. Finally, the paper concludes with a discussion of results and future research directions in section V.

II. BICOPTER DYNAMICS

Let $F_A = \{\hat{i}_A, \hat{j}_A, \hat{k}_A\}$ be an inertial frame and let $F_B = \{\hat{i}_B, \hat{j}_B, \hat{k}_B\}$ be a frame fixed to the bicopter \mathcal{B} as shown in Figure 1. The bicopter \mathcal{B} is constrained to move in the $\hat{i}_A - \hat{j}_A$ plane. Note that F_B is obtained by rotating it about the \hat{k}_A axis of F_A by θ , and thus

$$F_A \xrightarrow[3]{\theta} F_B. \quad (1)$$

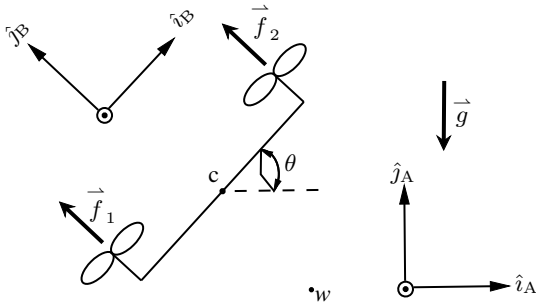


Fig. 1: Bicopter configuration considered in this paper. The bicopter is constrained to the $\hat{i}_A - \hat{j}_A$ plane and rotates about the \hat{k}_A axis of the inertial frame F_A .

Letting c denote the center of mass of the bicopter and w denote a fixed point on Earth, it follows from Newton's second law that

$$m \overset{A \bullet \bullet}{\vec{r}}_{c/w} = m \vec{g} + \vec{f}, \quad (2)$$

where m is the mass of the bicopter, \vec{g} is the acceleration due to gravity, and \vec{f} is the total force applied by the propellers to the bicopter. Letting $\vec{f}_1 = f_1 \hat{j}_B$ and $\vec{f}_2 = f_2 \hat{j}_B$ denote the forces applied by the two propellers, it follows that $\vec{f} = f_1 \hat{j}_B + f_2 \hat{j}_B$. Writing $\vec{r}_{c/w} = r_1 \hat{i}_A + r_2 \hat{j}_A$ yields

$$m \ddot{r}_1 = -(f_1 + f_2) \sin \theta, \quad (3)$$

$$m \ddot{r}_2 = (f_1 + f_2) \cos \theta - mg. \quad (4)$$

Next, it follows from Euler's equation that

$$\vec{J}_{B/c} \overset{A \bullet \bullet}{\vec{\omega}}_{B/A} = \vec{M}_{B/c}, \quad (5)$$

where $\vec{J}_{B/c}$ is the physical inertia matrix and $\vec{M}_{B/c}$ is the moment applied to \mathcal{B} about the point c . Note that $\vec{J}_{B/c} \overset{A \bullet \bullet}{\vec{\omega}}_{B/A} = J \ddot{\theta} \hat{k}_B$ and $\vec{M}_{B/c} = \ell(f_2 - f_1) \hat{k}_B$, where ℓ is the length of the bicopter arm, and thus it follows from (5) that

$$J \ddot{\theta} = \ell(f_2 - f_1). \quad (6)$$

Defining

$$F \triangleq f_1 + f_2, \quad (7)$$

$$M \triangleq (-f_1 + f_2)\ell, \quad (8)$$

it follows that

$$m \ddot{r}_1 = -F \sin \theta, \quad (9)$$

$$m \ddot{r}_2 = F \cos \theta - mg, \quad (10)$$

$$J \ddot{\theta} = M. \quad (11)$$

III. ADAPTIVE BACKSTEPPING CONTROL

In this section, we construct an adaptive backstepping controller to stabilize the bicopter system. To do so, the equations of motion, given by (9)-(11), must be reformulated into the strict feedback form to apply the classical backstepping. However, as shown below, the classical backstepping technique is not applicable due to the singularity of the input map.

A. Strict Feedback Form of Bicopter Dynamics

Defining

$$x_1 \triangleq \begin{bmatrix} r_1 \\ r_2 \\ \theta \end{bmatrix}, x_2 \triangleq \begin{bmatrix} \dot{r}_1 \\ \dot{r}_2 \\ \dot{\theta} \end{bmatrix}, u \triangleq \begin{bmatrix} F \\ M \end{bmatrix}, \Theta \triangleq \begin{bmatrix} m^{-1} \\ J^{-1} \end{bmatrix} \quad (12)$$

it follows that

$$\dot{x}_1 = x_2, \quad (13)$$

$$\dot{x}_2 = f_2(x_1, x_2) + g_2(x_1, x_2) \text{diag}(\Theta) u, \quad (14)$$

where

$$f_2(x_1, x_2) \triangleq \begin{bmatrix} 0 \\ -g \\ 0 \end{bmatrix}, \quad g_2(x_1, x_2) \triangleq \begin{bmatrix} -\sin(x_{1,3}) & 0 \\ \cos(x_{1,3}) & 0 \\ 0 & 1 \end{bmatrix}. \quad (15)$$

Note that the map g_2 is not invertible; hence, classical backstepping [20, p. 29] can not be applied to this system.

B. Dynamic Extension of Bicopter Dynamics

To circumvent the problem of the singularity of the input map, we extend the dynamics as shown below. Redefining

$$x_1 \triangleq \begin{bmatrix} r_1 \\ r_2 \end{bmatrix}, \quad x_2 \triangleq \begin{bmatrix} \dot{r}_1 \\ \dot{r}_2 \end{bmatrix}, \quad x_3 \triangleq \begin{bmatrix} F \\ \theta \end{bmatrix}, \quad x_4 \triangleq \begin{bmatrix} \dot{F} \\ \dot{\theta} \end{bmatrix}, \quad (16)$$

and

$$u \triangleq \begin{bmatrix} \ddot{F} \\ M \end{bmatrix}, \quad \Theta \triangleq \begin{bmatrix} \Theta_1 \\ \Theta_2 \end{bmatrix} = \begin{bmatrix} m^{-1} \\ J^{-1} \end{bmatrix}, \quad (17)$$

it follows from the equations of motion (3), (4), and (6) that

$$\dot{x}_1 = x_2, \quad (18)$$

$$\dot{x}_2 = f_2(x_1, x_2) + g_2(x_3)\Theta_1, \quad (19)$$

$$\dot{x}_3 = x_4, \quad (20)$$

$$\dot{x}_4 = \text{diag}(1, \Theta_2)u, \quad (21)$$

where

$$f_2(x_1, x_2) \triangleq \begin{bmatrix} 0 \\ -g \end{bmatrix}, \quad g_2(x_3) \triangleq \begin{bmatrix} -\sin(x_{3,2})x_{3,1} \\ \cos(x_{3,2})x_{3,1} \end{bmatrix}. \quad (22)$$

Note that the dynamic extension of the bicopter system, given by (18)-(21), is not in the desired strict feedback form. In fact, the extended dynamics is in pure feedback form since x_3 appears non-affinely in (19). However, since the input map $\text{diag}(1, \Theta_2)$ is invertible, and thus the backstepping technique can now be applied to the extended system to construct a controller.

C. Adaptive Backstepping-based Control of Bicopter

Next, we construct an adaptive controller based on the backstepping technique. This approach is based on the process described in [20, p. 29].

1) e_1 Stabilization: Let $x_{1d} = [r_{d1} \ r_{d2}]^T$ denote the desired trajectory, and define the tracking error $e_1 \triangleq x_1 - x_{1d}$. Consider the function

$$V_1 \triangleq \frac{1}{2}e_1^T e_1. \quad (23)$$

Differentiating (23) and using (18) yields

$$\dot{V}_1 = e_1^T \dot{x}_1 = e_1^T x_2. \quad (24)$$

Note that if $x_2 = -k_1 e_1$, where $k_1 > 0$, then $\dot{V}_1 < 0$. However, x_2 is not the control signal and thus can not be chosen arbitrarily. Instead, following the backstepping process, we design a control law that yields the desired x_2 response, as shown below.

2) e_2 Stabilization: Next, consider the function

$$V_2 \triangleq V_1 + \frac{1}{2}e_2^T e_2, \quad (25)$$

where

$$e_2 \triangleq x_2 - x_{2d}, \quad (26)$$

$$x_{2d} \triangleq -k_1 e_1. \quad (27)$$

Differentiating (25) and using (19) yields

$$\dot{V}_2 = -k_1 e_1^T e_1 + e_2^T \xi_2, \quad (28)$$

where

$$\xi_2 \triangleq x_1 + f_2 + g_2\Theta_1 + k_1 x_2. \quad (29)$$

Note that if

$$g_2(x_3)\Theta_1 = -e_2 - e_1 - f_2 - k_1 x_2, \quad (30)$$

then $\dot{V}_2 < 0$.

Let $\hat{\Theta}_1$ be an estimate of Θ_1 , and define $\tilde{\Theta}_1 \triangleq \hat{\Theta}_1 - \Theta_1$. Next, define

$$x_{3d} \triangleq x_3 - (g_2\tilde{\Theta}_1 + \xi_2) - k_2 e_2, \quad (31)$$

$$e_3 \triangleq x_3 - x_{3d}, \quad (32)$$

where $k_2 > 0$, which implies that

$$\xi_2 = e_3 - g_2\tilde{\Theta}_1 - k_2 e_2 \in \mathbb{R}^2. \quad (33)$$

Substituting (33) in (28) yields

$$\dot{V}_2 = -k_1 e_1^T e_1 - k_2 e_2^T e_2 + e_2^T \left(e_3 + g_2(\Theta_1 - \hat{\Theta}_1) \right). \quad (34)$$

3) Θ_1 Adaptation: Next, consider the function

$$V_2 \triangleq V_2 + \frac{1}{2}\gamma_1^{-1}(\Theta_1 - \hat{\Theta}_1)^T(\Theta_1 - \hat{\Theta}_1) \quad (35)$$

where $\gamma_1 > 0$. Differentiating (35) yields

$$\dot{V}_2 = -k_1 e_1^T e_1 - k_2 e_2^T e_2 + e_2^T e_3 + (\Theta_1 - \hat{\Theta}_1)^T \left(g_2^T e_2 - \gamma_1^{-1} \dot{\hat{\Theta}}_1 \right). \quad (36)$$

Letting

$$\dot{\hat{\Theta}}_1 = \gamma_1 g_2^T e_2 \quad (37)$$

yields

$$\dot{V}_2 = -k_1 e_1^T e_1 - k_2 e_2^T e_2 + e_2^T e_3. \quad (38)$$

4) e_3 Stabilization: Next, consider the function

$$V_3 \triangleq \mathcal{V}_2 + \frac{1}{2}e_3^T e_3. \quad (39)$$

Note that

$$\dot{\xi}_2 = x_2 + \mathcal{G}_2 \Theta_1 + k_1(f_2 + g_2 \Theta_1), \quad (40)$$

where

$$\mathcal{G}_2 \triangleq \partial_{x_3} g_2 = \begin{bmatrix} -\cos(x_{3,2})x_{3,1} & -\sin(x_{3,2}) \\ -\sin(x_{3,2})x_{3,1} & \cos(x_{3,2}) \end{bmatrix}. \quad (41)$$

Differentiating (39) and using (20), (31) and (40) yields

$$\dot{V}_3 = -k_1 e_1^T e_1 - k_2 e_2^T e_2 + e_3^T \xi_3 \quad (42)$$

where

$$\xi_3 \triangleq 2x_2 + k_1 e_1 + \mathcal{G}_2 x_4 \hat{\Theta}_1 + \gamma_1 g_2 g_2^T e_2 + \kappa_{12}(f_2 + g_2 \Theta_1) + k_1 k_2 x_2. \quad (43)$$

and $\kappa_{12} \triangleq k_1 - k_2$.

Let $\hat{\vartheta}_1$ be an estimate of Θ_1 , and define $\tilde{\vartheta}_1 \triangleq \hat{\vartheta}_1 - \Theta_1$. Next, define

$$x_{4d} \triangleq x_4 - (\kappa_{12} g_2 \tilde{\vartheta}_1 + \xi_3) - k_3 e_3, \quad (44)$$

where $k_3 > 0$, and $\hat{\vartheta}_1$ is given by the adaptation law (50). Rearranging (44) yields

$$\xi_3 = e_4 - \kappa_{12} g_2 \tilde{\vartheta}_1 - k_3 e_3 \in \mathbb{R}^2, \quad (45)$$

where

$$e_4 \triangleq x_4 - x_{4d}. \quad (46)$$

Substituting (45) in (42) yields

$$\dot{V}_3 = -k_1 e_1^T e_1 - k_2 e_2^T e_2 - k_3 e_3^T e_3 + e_3^T e_4 - e_3^T \kappa_{12} g_2 \tilde{\vartheta}_1. \quad (47)$$

5) ϑ_1 Adaptation: Next, consider the function

$$\mathcal{V}_3 \triangleq V_3 + \frac{1}{2}\gamma_2^{-1} \tilde{\vartheta}_1^T \tilde{\vartheta}_1, \quad (48)$$

where $\gamma_2 > 0$. Differentiating (48) yields

$$\dot{\mathcal{V}}_3 = -k_1 e_1^T e_1 - k_2 e_2^T e_2 - k_3 e_3^T e_3 + e_3^T e_4 - (\kappa_{12} g_2^T e_3 - \gamma_2^{-1} \dot{\tilde{\vartheta}}_1) \tilde{\vartheta}_1. \quad (49)$$

Letting

$$\dot{\tilde{\vartheta}}_1 = \gamma_2 \kappa_{12} g_2 (x_3)^T e_3, \quad (50)$$

yields

$$\dot{\mathcal{V}}_3 = -k_1 e_1^T e_1 - k_2 e_2^T e_2 - k_3 e_3^T e_3 + e_3^T e_4. \quad (51)$$

6) e_4 Stabilization: Next, consider the function

$$V_4 \triangleq \mathcal{V}_3 + \frac{1}{2}e_4^T e_4. \quad (52)$$

Differentiating (52) and using (21) yields

$$\dot{V}_4 = -k_1 e_1^T e_1 - k_2 e_2^T e_2 - k_3 e_3^T e_3 + e_4^T \xi_4, \quad (53)$$

where

$$\begin{aligned} \xi_4 \triangleq & \left(x_1 + 3f_2 + g_2 \hat{\Theta}_1 + 2k_1 x_2 \right. \\ & + k_2 (x_2 + k_1 e_1) + 2g_2 \Theta_1 \\ & + \frac{d}{dt} \left[\frac{\partial g(x_3)}{\partial x_3} \right] x_4 \hat{\Theta}_1 \\ & + \mathcal{G}_2 \text{diag}(1, \Theta_2) \hat{\Theta}_1 u + 2\mathcal{G}_2 x_4 \dot{\hat{\Theta}}_1 \\ & + \gamma_1 g_2 \left[x_4^T \mathcal{G}_2^T (x_2 + k_1 e_1) \right. \\ & \left. + g_2^T (f_2 + g_2 \Theta_1 + k_1 x_2) \right] \\ & + K_{12} \mathcal{G}_2 x_4 \hat{\vartheta}_1 \\ & + K_{12} g_2 \dot{\hat{\vartheta}}_1 + k_1 k_2 (f_2 + g_2 \Theta_1) \\ & \left. + k_3 \left(x_2 + \mathcal{G}_2 x_4 \hat{\Theta}_1 + g_2 \hat{\Theta}_1 \right. \right. \\ & \left. \left. + K_{12} (f_2 + g_2 \Theta_1) + k_1 k_2 x_2 \right) \right) \end{aligned} \quad (54)$$

where $K_{12} \triangleq k_1 + k_2$.

Note that if

$$\xi_4 = -k_4 e_4, \quad (55)$$

where $k_4 > 0$. Then,

$$\dot{V}_4 = -k_1 e_1^T e_1 - k_2 e_2^T e_2 - k_3 e_3^T e_3 - k_4 e_4^T e_4 < 0. \quad (56)$$

Let $\hat{\varphi}_1$ and $\hat{\Theta}_2$ be an estimate of Θ_1 and Θ_2 , respectively. Define $\tilde{\varphi}_1 \triangleq \hat{\varphi}_1 - \Theta_1$ and $\tilde{\Theta}_2 \triangleq \hat{\Theta}_2 - \Theta_2$. Then, letting

$$\begin{aligned} u = & - \left(\mathcal{G}_2 \text{diag}(1, \hat{\Theta}_2) \hat{\Theta}_1 \right)^{-1} \left(k_4 e_4 + e_3 \right. \\ & + (k_3(k_1 + k_2) + k_1 k_2 + 2 + \gamma_1 g_2 g_2^T) (f_2 + g_2 \hat{\varphi}_1) \\ & + (k_3(k_1 k_2 + 1) + k_1 + \gamma_1 g_2 g_2^T) x_2 \\ & + (\mathcal{G}_2 x_4 - k_3 g_2) \dot{\hat{\Theta}}_1 + \left(\frac{d}{dt} \mathcal{G}_2 + k_3 \mathcal{G}_2 \right) x_4 \hat{\Theta}_1 \\ & + K_{12} \mathcal{G}_2 x_4 \hat{\vartheta}_1 + K_{12} g_2 \dot{\hat{\vartheta}}_1 \\ & \left. + 2\gamma_1 \mathcal{G}_2 x_4 g_2^T (x_2 + k_1 e_1) \right), \end{aligned} \quad (57)$$

yields

$$\begin{aligned} \dot{V}_4 = & -k_1 e_1^T e_1 - k_2 e_2^T e_2 - k_3 e_3^T e_3 - k_4 e_4^T e_4 + e_4^T \cdot \\ & \left[- (k_3 K_{12} + k_1 k_2 + 2 + \gamma_1 g_2 \ g_2^T) g_2 \tilde{\varphi}_1 \right. \\ & \left. - \hat{\Theta}_1 \mathcal{G}_2 \begin{bmatrix} 0 \\ u_2 \end{bmatrix} \tilde{\Theta}_2 \right] \end{aligned} \quad (58)$$

7) $\hat{\varphi}_1$ and $\hat{\Theta}_2$ Adaptations: Next, consider the function

$$\mathcal{V}_4 = V_4 + \frac{1}{2} \gamma_3^{-1} \tilde{\varphi}_1^T \tilde{\varphi}_1 + \frac{1}{2} \gamma_4^{-1} \tilde{\Theta}_2^T \tilde{\Theta}_2, \quad (59)$$

where $\gamma_3 > 0$ and $\gamma_4 > 0$. Differentiating (59) yields

$$\begin{aligned} \dot{\mathcal{V}}_4 = & -k_1 e_1^T e_1 - k_2 e_2^T e_2 - k_3 e_3^T e_3 - k_4 e_4^T e_4 \\ & + \left(-e_4^T (k_3 K_{12} + k_1 k_2 + 2 + \gamma_1 g_2 \ g_2^T) g_2 + \gamma_3^{-1} \dot{\tilde{\varphi}}_1^T \right) \tilde{\varphi}_1 \\ & + \left(-e_4^T \hat{\Theta}_1 \mathcal{G}_2 \begin{bmatrix} 0 \\ u_2 \end{bmatrix} + \gamma_4^{-1} \dot{\tilde{\Theta}}_2^T \right) \tilde{\Theta}_2. \end{aligned} \quad (60)$$

Letting

$$\dot{\hat{\varphi}}_1 = \gamma_3 g_2^T (k_3 K_{12} + k_1 k_2 + 2 + \gamma_1 g_2^T g_2) e_4, \quad (61)$$

$$\dot{\hat{\Theta}}_2 = \gamma_4 \hat{\Theta}_1 \begin{bmatrix} 0 & u_2 \end{bmatrix} \mathcal{G}_2^T e_4, \quad (62)$$

yields

$$\dot{V}_4 = -k_1 e_1^T e_1 - k_2 e_2^T e_2 - k_3 e_3^T e_3 - k_4 e_4^T e_4. \quad (63)$$

The controller is thus given by (27), (31), (44), and (57) with the parameter adaption laws (37), (50), (61), and (62). The block diagram showing the architecture of the adaptive backstepping controller is shown in Figure 2.

D. Stability Analysis

Note that the control (57) requires $\mathcal{G}_2 \text{diag}(1, \hat{\Theta}_2) \hat{\Theta}_1$ to be nonsingular, which implies that \mathcal{G}_2 must be nonsingular and $\hat{\Theta}_1, \hat{\Theta}_2 \neq 0$. If $F \neq 0$, which is reasonably expected during the system's operation, \mathcal{G}_2 is nonsingular. However, the parameter adaptation laws do not ensure that $\hat{\Theta}_1, \hat{\Theta}_2 \neq 0$. Thus, the global asymptotic stability of the closed-loop system can not be guaranteed.

Next, consider the function

$$\begin{aligned} \mathcal{V}_4(e_1, e_2, e_3, e_4, \hat{\Theta}_1, \hat{\vartheta}_1, \hat{\varphi}_1, \hat{\Theta}_2) = & \frac{1}{2} e_1^T e_1 + \frac{1}{2} e_2^T e_2 \\ & + \frac{1}{2} e_3^T e_3 + \frac{1}{2} e_4^T e_4 + \frac{1}{2} \gamma_1^{-1} \tilde{\Theta}_1^T \tilde{\Theta}_1 + \frac{1}{2} \gamma_2^{-1} \tilde{\vartheta}_1^T \tilde{\vartheta}_1 \\ & + \frac{1}{2} \gamma_3^{-1} \tilde{\varphi}_1^T \tilde{\varphi}_1 + \frac{1}{2} \gamma_4^{-1} \tilde{\Theta}_2^T \tilde{\Theta}_2, \end{aligned} \quad (64)$$

where $\gamma_1, \gamma_2, \gamma_3, \gamma_4 > 0$. Let $D = \mathbb{R}^2 \times \mathbb{R}^2 \times \mathbb{R}^2 \times \mathbb{R}^2 \times \mathbb{R}/\{0\} \times \mathbb{R} \times \mathbb{R} \times \mathbb{R}/\{0\}$. Then, $\mathcal{V}_4(x) \geq 0$ for all $x \in D$. Furthermore, it follows from (63) that $\dot{\mathcal{V}}_4 \leq 0$. Moreover, $\dot{\mathcal{V}}_4(x) = 0$ if and only if $e_1 = e_2 = e_3 = e_4 = 0$. Let E be the set of all points in D

such that $e_1 = e_2 = e_3 = e_4 = 0$. Note that E is the largest positively invariant set with respect to (18)-(21) in E . Then, it follows from the Barbashin-Krasovskiy-La Salle's invariance principle [26] that $e_1, e_2, e_3, e_4 \rightarrow 0$.

IV. SIMULATIONS

In this section, we apply the adaptive backstepping controller developed in the previous section to the trajectory tracking problem. In particular, we use the adaptive controller to follow an elliptical and a second-order Hilbert curve based trajectory.

To simulate the bicopter, we assume that the mass of the bicopter is 1 kg and its inertia is 0.2 kg · m². In the controller, we set $k_1 = 5, k_2 = 5, k_3 = 4, \text{ and } k_4 = 4$. In the adaptation laws, we set the adaptation gains $\gamma_1 = 1, \gamma_2 = 0.05, \gamma_3 = 0.05, \text{ and } \gamma_4 = 0.1$, and the initial estimates $\hat{\Theta}_1(0) = 0.5, \hat{\vartheta}_1(0) = 0.5, \hat{\varphi}_1(0) = 0.5, \text{ and } \hat{\Theta}_2(0) = 40$.

A. Elliptical Trajectory

The bicopter is commanded to follow a elliptical trajectory given by

$$\begin{aligned} r_{d1}(t) = & 5 \cos(\phi) - 5 \cos(\phi) \cos(\omega t) - 3 \sin(\phi) \sin(\omega t), \\ r_{d2}(t) = & 5 \sin(\phi) - 5 \sin(\phi) \cos(\omega t) + 3 \cos(\phi) \sin(\omega t), \end{aligned}$$

where $\phi = 45 \text{ deg}$ and $\omega = 0.3 \text{ rad/s}^{-1}$. Figure 3 shows the trajectory-tracking response of the bicopter, where the desired trajectory is shown in black dashes and the output trajectory response is shown in blue. Figure 4 shows the position r_1, r_2 response and the roll angle θ response of the bicopter with the adaptive backstepping controller. Figure 5 shows the norm of the position errors obtained with the adaptive backstepping controller on a logarithmic scale.

Figure 6 shows the estimates $\hat{\Theta}_1, \hat{\vartheta}_1, \text{ and } \hat{\varphi}_1$ of Θ_1 and the estimate $\hat{\Theta}_2$ of Θ_2 . Note that the parameter estimates do not converge to their actual values. However, the non-convergence of the estimates is not due to persistency-related issues. In the adaptive controller design, since the parameter adaptation laws are chosen to cancel undesirable factors and not to estimate the parameters, the estimates do not necessarily need to converge. Finally, Figure 7 shows the control u generated by the adaptive backstepping controller (57) and the corresponding forces f_1 and f_2 . Note that the forces f_1, f_2 are computed using (7), and (8).

B. Hilbert trajectory

Next, the bicopter is commanded to follow a non-smooth trajectory constructed using a second-order Hilbert curve. The trajectory is constructed using the algorithm described in Appendix A of [27] with a maximum velocity $v_{\max} = 1 \text{ m/s}$ and a maximum acceleration $a_{\max} = 1 \text{ m/s}^2$. Figure 8 shows the

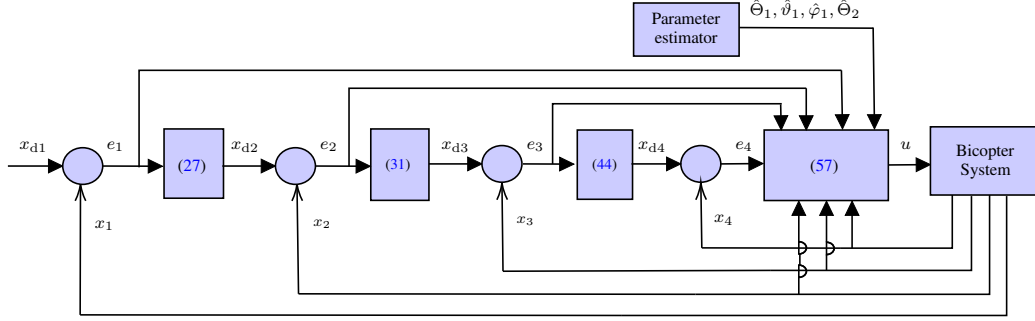


Fig. 2: Adaptive backstepping control architecture.

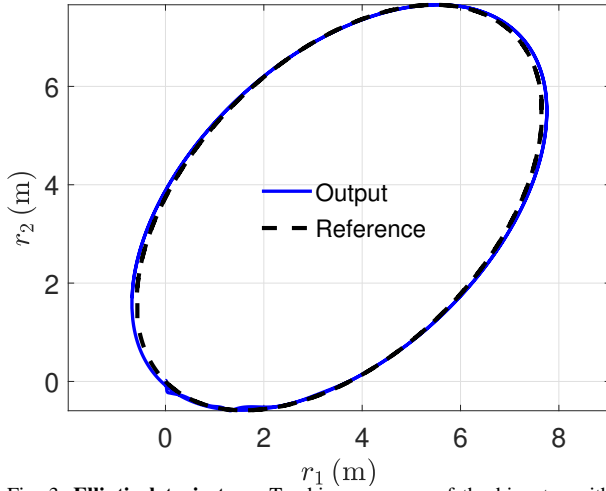


Fig. 3: **Elliptical trajectory.** Tracking response of the bicopter with the adaptive backstepping controller. Note that the output trajectory is shown in solid blue, and the reference trajectory is in dashed black.

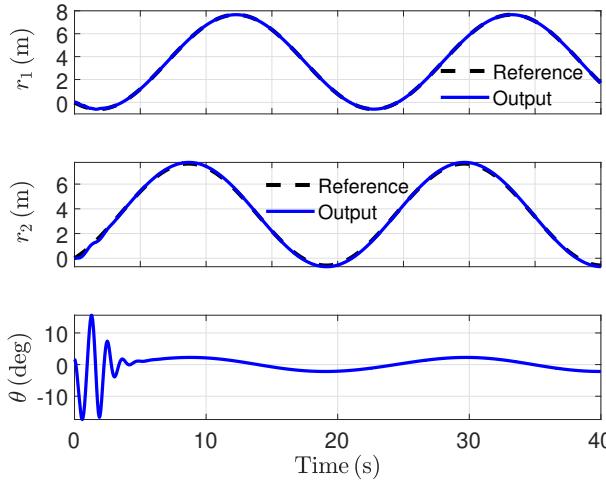


Fig. 4: **Elliptical trajectory.** Position (r_1, r_2) and roll angle θ response of the bicopter obtained with adaptive backstepping controller (57).

trajectory-tracking response of the bicopter, where the desired trajectory is shown in black dashes, and the output trajectory response is shown in blue. Figure 9 shows the position r_1 and r_2 response and the roll

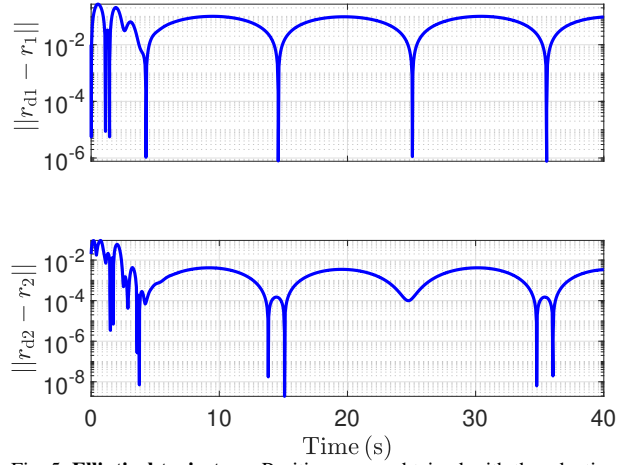


Fig. 5: **Elliptical trajectory.** Position errors obtained with the adaptive backstepping controller (57) on a logarithmic scale.

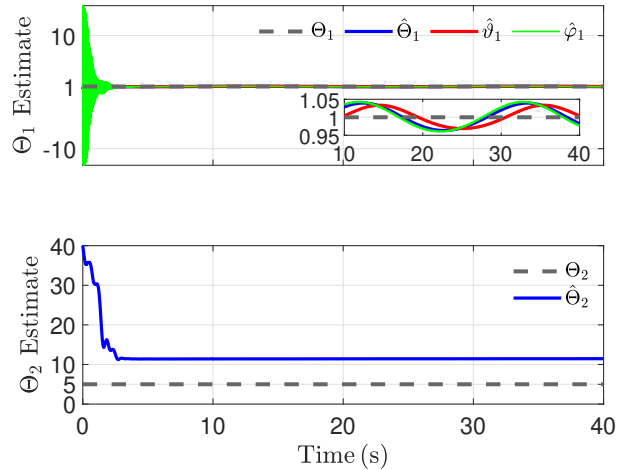


Fig. 6: **Elliptical trajectory.** Estimates of Θ_1 and Θ_2 obtained with adaption laws (37), (50), (61), and (62).

angle θ response of the bicopter with the adaptive backstepping controller. Figure 10 shows the norm of the position errors obtained with the adaptive backstepping controller on a logarithmic scale.

Figure 11 shows the estimates $\hat{\Theta}_1$, $\hat{\vartheta}_1$, and $\hat{\varphi}_1$ of Θ_1 and the estimate $\hat{\Theta}_2$ of Θ_2 . As in the previous case,

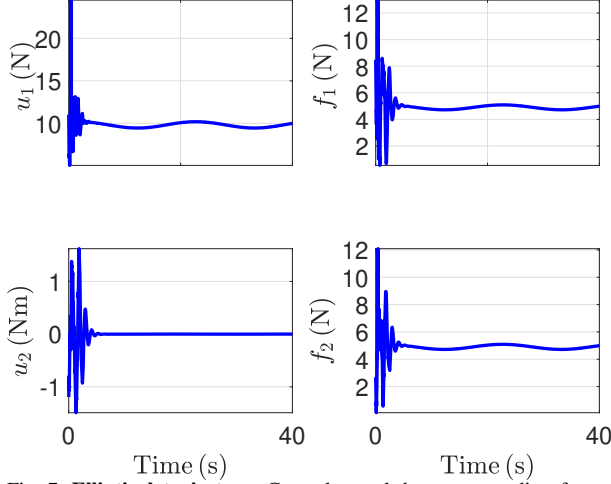


Fig. 7: **Elliptical trajectory**. Control u and the corresponding forces f_1 and f_2 obtained with adaptive backstepping controller (57).

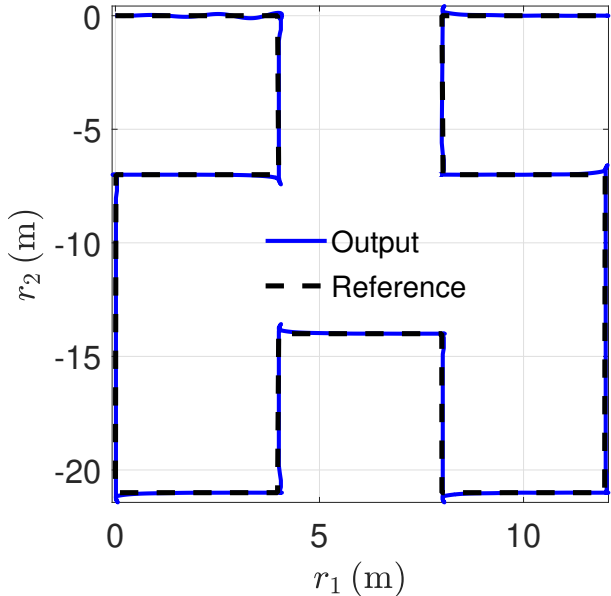


Fig. 8: **Hilbert trajectory**. Tracking response of the bicopter with adaptive backstepping controller. Note that the output trajectory is in solid blue, and the desired trajectory is in dashed black.

note that the estimates do not converge to their actual values. Finally, Figure 12 shows the control u generated by the adaptive backstepping controller (57), and the corresponding forces f_1 and f_2 . Note that the forces f_1 and f_2 are computed using (7), and (8).

The preceding two examples show that the adaptive backstepping controller stabilizes the bicopter dynamics and successfully tracks the desired trajectory without prior knowledge of the bicopter dynamics.

V. CONCLUSIONS

This paper presented an adaptive backstepping-based controller for the stabilization and tracking problem in a bicopter system. It is shown that the backstepping

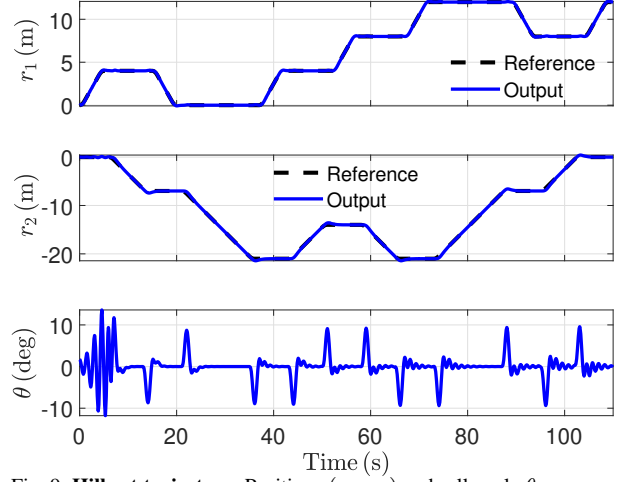


Fig. 9: **Hilbert trajectory**. Positions (r_1, r_2) and roll angle θ response of the bicopter with adaptive backstepping controller.

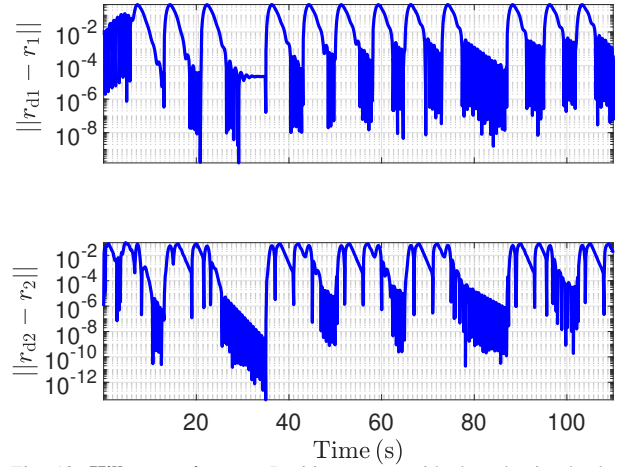


Fig. 10: **Hilbert trajectory**. Position errors with the adaptive backstepping controller on a logarithmic scale.

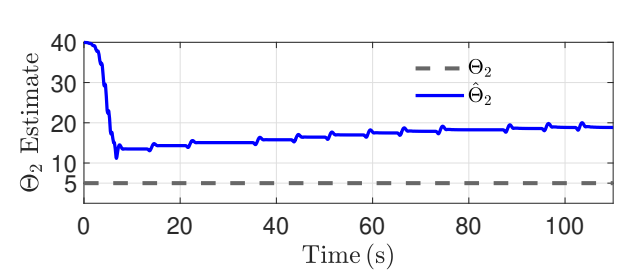
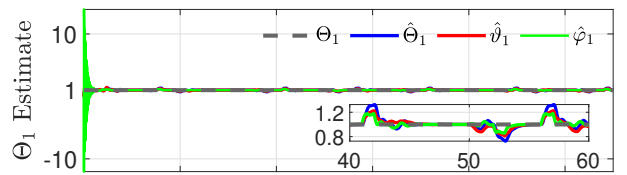


Fig. 11: **Hilbert trajectory**. Θ_1 and Θ_2 Estimations with the adaptive backstepping controller. Note that the parameters used in the model are in dashed black.

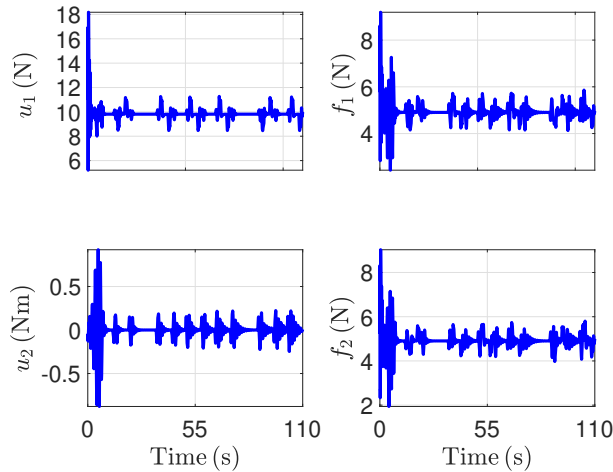


Fig. 12: **Hilbert trajectory.** Control u and the corresponding forces f_1 and f_2 obtained with adaptive backstepping controller.

process can not be applied to the bicopter dynamics due to the singularity of the input map. The bicopter dynamics is then dynamically extended to circumvent the singularity problem. The backstepping process is then used to stabilize the successive states of the extended bicopter system and design parameter adaption laws. Since the final control law requires the inversion of two of the parameter estimates, the global asymptotic stability of the closed-loop system cannot be guaranteed as the adaptation laws do not enforce a constraint on the estimate values. However, as shown in the numerical simulations, the closed-loop system is asymptotically stable with appropriately chosen gains, and the controller yields the desired tracking performance.

Future extensions will focus on 1) integrating constraints in the parameter adaption law that guarantees global stability of the closed-loop system for all gains chosen in the control law and the parameter adaptation laws, 2) reformulating the control laws as cascaded control, and finally, 3) extending the adaptive backstepping control presented in this paper to design a stabilizing and tracking controller for a quadcopter.

REFERENCES

- [1] A. Mukherjee, S. Misra, and N. S. Raghuvanshi, "A survey of unmanned aerial sensing solutions in precision agriculture," *J. Netw. Comput. Appl.*, vol. 148, p. 102461, 2019.
- [2] A. Lucieer, S. M. d. Jong, and D. Turner, "Mapping landslide displacements using Structure from Motion (SfM) and image correlation of multi-temporal UAV photography," *Prog. Phys. Geogr.*, vol. 38, no. 1, pp. 97–116, 2014.
- [3] V. V. Klemas, "Coastal and environmental remote sensing from unmanned aerial vehicles: An overview," *J. Coast. Res.*, vol. 31, no. 5, pp. 1260–1267, 2015.
- [4] Y. Li and C. Liu, "Applications of multirotor drone technologies in construction management," *Int. J. Constr. Manag.*, vol. 19, no. 5, pp. 401–412, 2019.
- [5] D. K. Villa, A. S. Brandao, and M. Sarcinelli-Filho, "A survey on load transportation using multirotor UAVs," *J. Intell. Robot. Syst.*, vol. 98, pp. 267–296, 2020.
- [6] T. P. Nascimento and M. Saska, "Position and attitude control of multirotor aerial vehicles: A survey," *Annu. Rev. Contr.*, vol. 48, pp. 129–146, 2019.
- [7] J. A. Marshall, W. Sun, and A. L'Afflitto, "A survey of guidance, navigation, and control systems for autonomous multi-rotor small unmanned aerial systems," *Annu. Rev. Contr.*, vol. 52, pp. 390–427, 2021.
- [8] P. Castillo, A. Dzul, and R. Lozano, "Real-time stabilization and tracking of a four-rotor mini rotorcraft," *IEEE Trans. Contr. Sys. Tech.*, vol. 12, no. 4, pp. 510–516, 2004.
- [9] B. J. Emran and H. Najjaran, "A review of quadrotor: An underactuated mechanical system," *Annu. Rev. Contr.*, vol. 46, pp. 165–180, 2018.
- [10] R. Amin, L. Aijun, and S. Shamshirband, "A review of quadrotor UAV: Control methodologies and performance evaluation," *Int. J. Autom. Contr.*, vol. 10, no. 2, pp. 87–103, 2016.
- [11] B. Whitehead and S. Bieniawski, "Model reference adaptive control of a quadrotor UAV," in *AIAA Guid. Nav. Contr. Conf. Ex.*, 2010, p. 8148.
- [12] Z. T. Dydek, A. M. Annaswamy, and E. Lavretsky, "Adaptive control of quadrotor UAVs: A design trade study with flight evaluations," *IEEE Trans. Contr. Sys. Tech.*, vol. 21, no. 4, pp. 1400–1406, 2012.
- [13] Z. Zuo and P. Ru, "Augmented L1 adaptive tracking control of quadrotor unmanned aircrafts," *IEEE. Trans. Aerosp. Elec. Sys.*, vol. 50, no. 4, pp. 3090–3101, 2014.
- [14] T. Espinoza-Fraire, A. Saenz, F. Salas, R. Juarez, and W. Giernacki, "Trajectory tracking with adaptive robust control for quadrotor," *Applied Sciences*, vol. 11, no. 18, p. 8571, 2021.
- [15] Z. Wu, S. Cheng, K. A. Ackerman, A. Gahlawat, A. Lakshmanan, P. Zhao, and N. Hovakimyan, "L1 adaptive augmentation for geometric tracking control of quadrotors," in *2022 International Conference on Robotics and Automation (ICRA)*, IEEE, 2022, pp. 1329–1336.
- [16] O. Mofid and S. Mobayen, "Adaptive sliding mode control for finite-time stability of quad-rotor UAVs with parametric uncertainties," *ISA trans.*, vol. 72, pp. 1–14, 2018.
- [17] A. Goel, J. A. Paredes, H. Dadhaniya, S. A. Ul Islam, A. M. Salim, S. Ravela, and D. Bernstein, "Experimental implementation of an adaptive digital autopilot," in *Proc. Amer. Contr. Conf.*, 2021, pp. 3737–3742.
- [18] J. Spencer, J. Lee, J. A. Paredes, A. Goel, and D. Bernstein, "An adaptive PID autotuner for multicopters with experimental results," in *Proc. Int. Conf. Rob. Autom.*, IEEE, 2022, pp. 7846–7853.
- [19] PX4 User Guide, *Multicopter Control Architecture*, https://docs.px4.io/main/en/flight_stack/controller_diagrams.html [Online; accessed 26 February 2023].
- [20] M. Krstić, P. V. Kokotović, and I. Kanellakopoulos, *Nonlinear and Adaptive Control Design*. John Wiley & Sons, 1995.
- [21] J. Descusse and C. H. Moog, "Decoupling with dynamic compensation for strong invertible affine non-linear systems," *International Journal of Control*, vol. 42, no. 6, pp. 1387–1398, 1985.
- [22] S. Zhang and W. Qian, "Dynamic backstepping control for pure-feedback nonlinear systems," *Computing Research Repository*, vol. abs/1706.08641, 2017. arXiv: 1706.08641. [Online]. Available: <http://arxiv.org/abs/1706.08641>.
- [23] F. Mazenc, L. Burlion, and M. Malisoff, "Backstepping design for output feedback stabilization for a class of uncertain systems using dynamic extension," in *2nd IFAC Conference on Modelling, Identification and Control of Nonlinear Systems*, 2018, pp. 260–265.
- [24] J. Reger and L. Triska, "Dynamic extensions for exact backstepping control of systems in pure feedback form," in *58th IEEE Conference on Decision and Control*, 2019, pp. 480–486.
- [25] L. Triska, J. Portella, and J. Reger, "Dynamic extension for adaptive backstepping control of uncertain pure-feedback systems," *IFAC-PapersOnLine*, vol. 54, no. 14, pp. 307–312, 2021.
- [26] H. K. Khalil, *Nonlinear Systems*. Pearson, 2013.
- [27] J. Spencer, J. Lee, J. A. Paredes, A. Goel, and D. Bernstein, "An adaptive pid autotuner for multicopters with experimental results," in *2022 International Conference on Robotics and Automation (ICRA)*, IEEE, 2022, pp. 7846–7853.